Atmospheric Environment 197 (2019) 66–76

Contents lists available at ScienceDirect

Atmospheric Environment

journal homepage: www.elsevier.com/locate/atmosenv

# Glaciochemical records for the past century from the Qiangtang Glacier No.1 ice core on the central Tibetan Plateau: Likely proxies for climate and atmospheric circulations

Cheng Wang[a,b], Lide Tian[a,c,d,*], Lili Shao[a,b], Yao Li[a,b]

[a] Key Laboratory of Tibetan Environment Changes and Land Surface Processes, Institute of Tibetan Plateau Research, Chinese Academy of Science (CAS), Beijing, 100101, China
[b] University of Chinese Academy of Science, Beijing, 100049, China
[c] Institute of International Rivers and Eco-Security, Yunnan University, Kunming, 650091, China
[d] CAS Center for Excellence in Tibetan Plateau Earth Sciences, Beijing, 100101, China

ARTICLE INFO

*Keywords:*
Qiangtang ice core
Glaciochemical records
Climate change
Central Tibetan Plateau

ABSTRACT

Previous studies of glaciochemical records retrieved from the southern and northern sectors of the Tibetan Plateau (TP) have revealed that there are diverse patterns of climate change within this region. However, uncertainty remains regarding changes in the atmospheric environment over the central TP where the Indian monsoonal circulation and westerly winds meet. This study presents a glaciochemical record of the past 112 years from the upper part of the ice core drilled into the Qiangtang Glacier No.1 (QT-1) located in the central TP. The purpose of this study is to understand the glaciochemical controls, if any, and how these controls have been affected by both local climate parameters and atmospheric circulation patterns. An empirical orthogonal function (EOF) analysis was performed to determine the significance of any chemical components. The results show that the major soluble ions ($Na^+$, $K^+$, $Mg^{2+}$, $Ca^{2+}$, $Cl^-$, $NO_3^-$, $NH_4^+$ and $SO_4^{2-}$) are predominantly controlled by crustal aerosols and have high loadings on EOF1. Correlation analysis between EOF1 and the annual dust-event frequency recorded by local/regional meteorological stations suggests that the ice core chemical record provides a reasonable proxy for local/regional atmospheric dust loading. Analysis of EOF1 also demonstrates changes that are consistent with regional meteorological parameters and large-scale circulations, revealing a strong link with the glaciochemical record. The windy, cold-dry climate and/or enhanced northwesterly/westerly winds appear to be responsible for the higher atmospheric dust aerosols, leading to higher concentrations of ions. Our analysis also isolated a significant positive correlation between EOF1 and the Pacific Decadal Oscillation (PDO) index, suggesting that, as an underlying mechanism, the PDO likely influences the regional climate conditions and atmospheric circulation patterns and thereby the QT-1 ion records. Our findings may, therefore, enhance the understanding of the relationship between chemical records and climatological variations that are preserved in ice cores, improve our knowledge of changes in the composition of the atmosphere and atmospheric circulation over the central TP, and potentially facilitate reconstruction of the paleo-PDO.

## 1. Introduction

Ice core records are recognized as valuable tools for reconstructing both the paleoclimate and the paleoenvironment (Dansgaard et al., 1993; Thompson et al., 1998; Davis et al., 2005). It has been suggested that high-resolution ice cores extracted from judiciously selected sites can provide both a long-term perspective on the variability of meteorological elements (such as precipitation and temperature) (Thompson et al., 1985; Thompson et al., 2013) and past atmospheric conditions (Thompson et al., 2000; Kaspari et al., 2007; Grigholm et al., 2015; Grigholm et al., 2017). The direct and detailed records of paleoclimatic change retrieved from ice cores can, therefore, improve the understanding of the mechanisms that drive climate change and improve the performance of climate models (Gao et al., 2008; Osterberg et al., 2017).

Since the major ions ($Na^+$, $K^+$, $Mg^{2+}$, $Ca^{2+}$, $Cl^-$, $NO_3^-$, $NH_4^+$ and

* Corresponding author. The Institute of Tibetan Plateau Research, Chinese Academy of Sciences, 3rd Building, 16 Lincui Rd, Chaoyang District, Beijing, 100101, China.
*E-mail address:* ldt@itpcas.ac.cn (L. Tian).

https://doi.org/10.1016/j.atmosenv.2018.10.028
Received 5 June 2018; Received in revised form 17 October 2018; Accepted 18 October 2018
Available online 19 October 2018
1352-2310/ 

$SO_4^{2-}$) found in ice cores have different emission sources (*e.g.*, dust, marine, biogenic and anthropogenic emissions) and are also influenced by local/regional environments or transport pathways (Wake et al., 1993; Legrand and Mayewski, 1997; Kang et al., 2000), they have the potential to provide unique records of paleoclimatic change or regional atmospheric circulations (Yao et al., 2004; Grigholm et al., 2009; Cui et al., 2014; Grigholm et al., 2015). Over the past few decades, many efforts have been made to reconstruct paleoenvironmental conditions from glaciochemical records retrieved from the Tibetan Plateau (TP). A number of studies have found that concentrations of major ions (such as $Na^+$, $K^+$, $Mg^{2+}$, $Ca^{2+}$ and $Cl^-$) preserved in ice cores from the northern and western margins of the TP can be used as indicators of mineral dust input (Wake et al., 1990; Yao et al., 2004), due to the close proximity of these locations to the vast arid and semiarid regions of central Asia. However, with the increasing impact of human activity on the atmosphere, some ions (*e.g.*, $NH_4^+$, $NO_3^-$, $K^+$ and $SO_4^{2-}$) offer the potential to detect anthropogenic input from livestock wastes, energy consumption and fertilizers (Zhao et al., 2008; Zhao et al., 2011; Grigholm et al., 2017).

On the southern margins of the TP, major ions come from two main sources: marine aerosols and crustal aerosols (Shrestha et al., 2002; Li et al., 2007; Xu et al., 2014). $Na^+$ and $Cl^-$ ions are mainly marine aerosols sourced from the Arabian Sea and the Bay of Bengal and are transported inland by the Asian Monsoon. Therefore, $Na^+$ and $Cl^-$ ions are reliable proxies of the intensity of the Asian Monsoon (Wake et al., 1990; Wake et al., 1993; Shrestha et al., 1997). Ionic records from the arid regions of central and southern Asia appear to be related to the predominance of continental air masses (Wake et al., 1993; Xu et al., 2014). The concentrations of $NH_4^+$, $NO_3^-$, $K^+$, and $SO_4^{2-}$ also provide information about changes in regional anthropogenic sources (Hou et al., 2003; Duan et al., 2007; Zhao et al., 2011; Grigholm et al., 2017). Moreover, there is evidence that glaciochemical records in ice cores can reflect shifts in atmospheric circulation patterns (Wake et al., 1993; Kang et al., 2002; Kaspari et al., 2007). For example, the East Rongbuk ice core record revealed that the majority of the crustal species are related to winter atmospheric circulation patterns and that the remainder of the crustal species in the core are related to summer atmospheric circulation patterns (Kang et al., 2002).

Compared with studies of ice cores from the southern and northern TP, there is a gap in the understanding of the chemical composition of the atmosphere in the transboundary region. Therefore, ice cores were drilled on Qiangtang Glacier No.1 (QT-1) in the central TP, a glacier located on the eastern slope of the Awu Mountains (Fig. 1). Earlier studies suggested that interannual oxygen isotope ($\delta^{18}O$) variations in this core appeared to be controlled by large-scale atmospheric circulations associated with the El Niño Southern Oscillation cycle, rather than by local meteorological conditions (Shao et al., 2017). The extent to which local meteorological conditions and atmospheric circulation patterns influence the ion concentrations in this ice core remains unclear.

Here, we present a 112-year (1900–2011) major soluble ion record constructed from the analysis of the QT-1 ice core. We performed an EOF analysis of the major ions and compared our results to the regional meteorological parameters and large-scale atmospheric circulation patterns. The purpose of this study was to reveal the relations between the glaciochemical records extracted from a central TP ice core and local/regional meteorological variables and atmospheric circulation patterns.

## 2. Methodology

### 2.1. Acquisition of the ice core

QT-1 Glacier is located in the mid-TP. At the collection site, the glacier has a width of about 1 km and length of 2 km. Ground Penetrating Radar measurement shows its thickness is 109 m in summit and the deepest site is over 132 m. The annual air temperature is −10.8 °C at the col of the glacier near the core site based on the automatic weather station (AWS). The annual precipitation is about 315 mm observed by the AWS located about 20 km away from the glacier. In May 2014, two ice cores were drilled as far as the bedrock on the saddle of QT-1 (33.30°N, 88.69°E, 5890 m above sea level (asl)) (Fig. 1). The ice core samples were kept frozen and transported to a laboratory freezer in Lhasa. The upper 19.52 m of the 108.88 m ice core was cut into 643 contiguous samples at intervals of 2.5–4 cm. The outer 2 cm annulus was scraped off each of the samples using a clean stainless-steel scalpel. The inner ice discs were then placed into pre-cleaned high-density polyethylene containers prior to glaciochemical analysis.

### 2.2. Chemical analyses

Prior to analysis, the samples were removed from the laboratory freezer and allowed to thaw naturally at room temperature. The major cations ($Na^+$, $NH_4^+$, $K^+$, $Mg^{2+}$ and $Ca^{2+}$) and anions ($Cl^-$, $NO_3^-$ and $SO_4^{2-}$) were determined using Dionex ion chromatograph models ICS2000 and ICS2005 at the Key Laboratory of Tibetan Environment Change and Land Surface Processes, Institute of Tibetan Plateau Research, Chinese Academy of Sciences (ITPCAS). Cations were analysed using a Dionex CS12A 4 mm separatory column with a CS12A 4 mm guard column using 20 mM MSA eluent, and anions was analysed by ICS2500 with AsII-HC column, 25 mM KOH eluent and ASRS suppresser. The detection limits for the cation and anion measurements were 1 ng/g. Field blank analyses showed that contamination during sampling, transport and treatment was negligible.

### 2.3. Dating of the core

The 19.52 m core was dated by identifying annual signals, and the results were confirmed by measuring radioactive ($^{137}Cs$) layers. Dating was completed by determining the seasonal $\delta^{18}O$ and d-excess fluctuation values and combining the results with seasonal variations in microparticles. The dating results were calibrated using the 1963 tritium peak at a depth of ~9.2 m. Accordingly, the 19.52 m core was dated to between 1900 and 2011 CE (~6 samples/year) and the absolute accuracy of the dating was ± 2 years. The analytical procedures for the $\delta^{18}O$ and ice core dating processes have been described in detail elsewhere (Shao et al., 2017).

### 2.4. Meteorological data

To assess the relationship between meteorological conditions and the ion concentration record, we used local/regional meteorological data from the meteorological stations at Shiquanhe, Gaize, Amdo, Baingoin and Shenzha (China Meteorological Data Service Center, http://data.cma.cn/). These stations are in close proximity to the QT-1 ice core site (Fig. 1).

The National Center for Environmental Prediction and National Center for Atmospheric Research (NCEP/NCAR) have provided a reanalysis of global climate data since 1948 for locations where long continuous datasets are available (https://www.esrl.noaa.gov/psd/data/gridded/data.ncep.reanalysis.html). In this study, we used 400 hPa wind data from the NCEP/NCAR reanalysis to investigate potential associations between the glaciochemical records and atmospheric circulation patterns.

The Pacific Decadal Oscillation (PDO) index, first introduced by Mantua et al. (1997), is characterized by the delineation of a leading EOF of monthly mean anomalies of sea surface temperatures (SSTs) found in the North Pacific Ocean (NPO; 20°-70°N) (Newman et al., 2016). During its positive phase, the PDO warms the eastern areas of the NPO and cools the western and central areas of the NPO, and *vice versa*. In this study, we used digital values from the PDO index as recorded in the Mantua's ftp directory (http://research.jisao.washington.

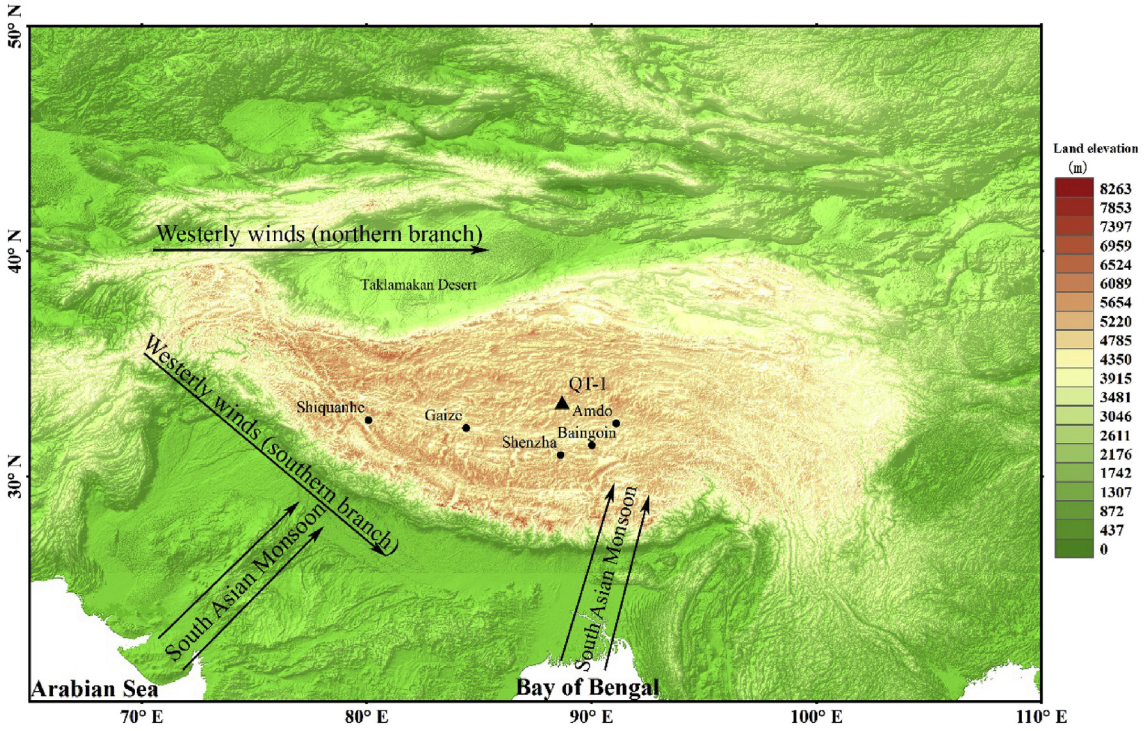


**Fig. 1.** Map showing the QT-1 ice core drill site and the surrounding meteorological stations. The black triangle represents the QT-1 site; the green dots are the surrounding meteorological stations. (For interpretation of the references to colour in this figure legend, the reader is referred to the Web version of this article.)

edu/pdo/PDO.latest.txt).

The Dynamic Normalized Seasonality (DNS) Index is based on the intensity of the normalized seasonality of any particular wind field; however, monsoonal circulations are characterized by strong seasonal variations. Therefore, to indicate the summer monsoonal intensity in this study, we used the South Asian Summer Monsoon Index (SASMI), which is defined as an area-averaged seasonally (JJAS) DNS at 850 hPa within the South Asian domain (5°-22.5°N, 35°-97.5°E) (Li and Zeng, 2002; Li and Zeng, 2003).

### 2.5. Statistical analysis

Empirical orthogonal function (EOF) analysis allows a robust assessment of the relationships between several variates and provides new time series that represent these relations through analysis of the covariance structure of its variates (Meeker et al., 1995). In this study, EOF analysis provided common variations in the concentrations of major ions over the past century and also yielded a new time series representing the relationships between them.

## 3. Results and discussion

### 3.1. Time series of major soluble ions

Table 1 provides a statistical summary of the major ion ($NO_3^-$, $SO_4^{2-}$, $Cl^-$, $K^+$, $Mg^{2+}$, $NH_4^+$, $Ca^{2+}$ and $Na^+$) concentrations in the QT-1 ice core. $Ca^{2+}$ is the dominant ion, with a mean concentration of approximately 961 ng/g that, on average, accounts for nearly half of the total calculated ion loading. Such high $Ca^{2+}$ concentrations are usually an indicator of dust that originated from arid and semiarid areas surrounding the ice core site (Wake et al., 1990). Fig. 2 shows a time series of the annual concentrations of major soluble ions that displays very similar trends over the period from 1900 to 2011, despite diverse variations in concentration observed for specific ions. All of the major ion concentrations have different magnitudes of fluctuation but lack long-term trends. We noted some dramatic increases in each of the annual ion concentrations in the 1930s, 1950s, 1960s, 1970s and 1980s that alternated with periods of relatively low concentrations. We compared descriptions of the dust layer for this ice core with the ion concentration variations and confirmed that the high-frequency dust layers match the ion concentration peaks.

We subsequently performed EOF analysis on the major ions (Table 2). The results indicated that EOF1 accounted for 70.8% of the total variance in the major ion concentrations and that almost all of the major ions had high loadings on EOF1, similar to the EOF associations derived from samples from the Mt. Geladaindong ice core (Kang et al., 2010). The strong associations between the major ions would suggest that these ions have a common source and/or similar atmospheric transport pathways. Atmospheric aerosols are usually dominated by crustal aerosols in remote continental regions, such as the TP, that have

**Table 1**
Mean, maximum (Max.), minimum (Min.), median, and standard deviation (SD) values of the major soluble ion concentrations in the QT-1 ice core (ng/g). The analytical detection limit was 1 ng/g for all the ions.

| | $NO_3^-$ | $SO_4^{2-}$ | $Cl^-$ | $K^+$ | $Mg^{2+}$ | $NH_4^+$ | $Ca^{2+}$ | $Na^+$ |
|---|---|---|---|---|---|---|---|---|
| Mean | 260.02 | 351.22 | 208.30 | 28.97 | 75.51 | 160.43 | 961.10 | 181.86 |
| Max. | 725.84 | 1002.73 | 590.45 | 83.97 | 211.78 | 423.69 | 2662.62 | 519.58 |
| Min. | 29.49 | 29.65 | 59.84 | 8.64 | 17.35 | 43.95 | 159.02 | 41.76 |
| Median | 229.46 | 320.20 | 190.22 | 25.96 | 69.42 | 150.06 | 791.95 | 150.54 |
| SD | 156.85 | 237.89 | 104.14 | 12.39 | 39.27 | 77.52 | 597.58 | 108.34 |

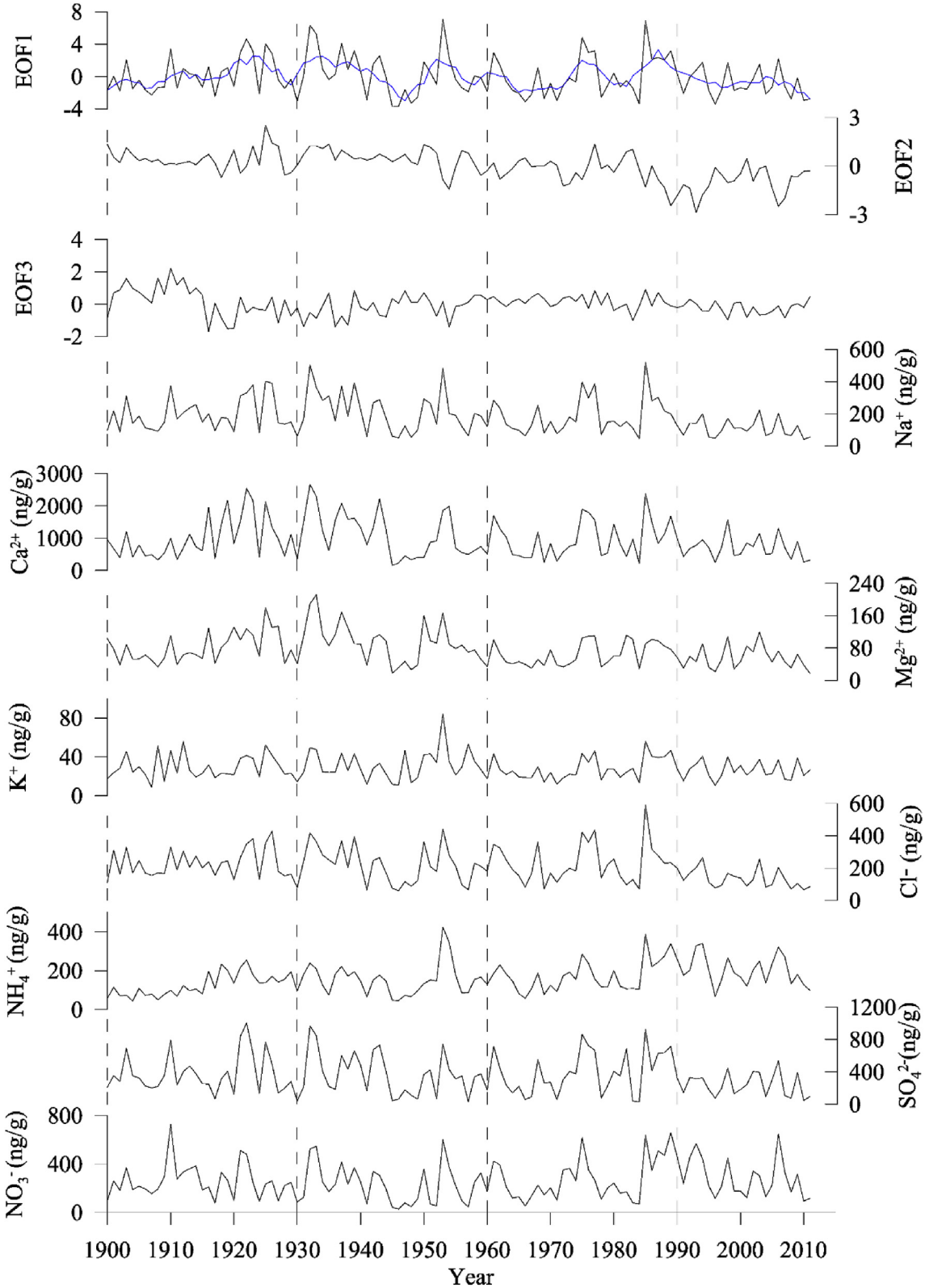


**Fig. 2.** Time-series of EOF and annual concentrations of major soluble ions from the QT-1 core. The blue line represents a time series of 5-year running means. (For interpretation of the references to colour in this figure legend, the reader is referred to the Web version of this article.)

minimal anthropogenic inputs (Li et al., 2007), indicating that the aerosols isolated from the QT-1 ice core are likely derived from crustal dust and/or rocks. Some sedimentary minerals, such as calcite, dolomite, gypsum, anhydrite, halite and potassium/magnesium salts, are commonly found in the QT-1 region (Li et al., 2007; Grigholm et al., 2009; Zheng et al., 2016) and therefore provide potential sources of major soluble ions. Since the mineral aerosols in this region are transported by the movement of continental air masses (Kang et al., 2002), the EOF1 may potentially indicate the occurrence, and behaviour, of dust storm events. The timing of EOF2, which represents 10.6% of the

**Table 2**
Results from the EOF analysis for a time series of major ions. The numbers in the table represent the percentage (%) of variance associated with each major ion. Negative values represent an inverse relationship. 'Total' represents the percentage (%) of total variance in the major ion records explained by each EOF.

| | EOF1 | EOF2 | EOF3 |
|---|---|---|---|
| $NO_3^-$ | 80.8 | 46.2 | −18.4 |
| $SO_4^{2-}$ | 90.9 | −3.0 | −15.4 |
| $NH_4^+$ | 69.5 | 61.4 | 30.2 |
| $Cl^-$ | 90.1 | −12.3 | −18.9 |
| $K^+$ | 80.3 | −6.0 | −19.7 |
| $Mg^{2+}$ | 78.0 | −42.5 | 34.1 |
| $Ca^{2+}$ | 87.4 | −9.4 | 35.6 |
| $Na^+$ | 93.3 | −21.3 | −18.1 |
| Total | 70.8 | 10.6 | 6.2 |

total variance, differs from dust-related species. EOF2 loadings are dominated by $NH_4^+$ and $NO_3^-$ and possibly represent unique biogenic sources related to agricultural activities (Mayewski et al., 1983; Shrestha et al., 1997). The aerosols produced, mainly $NH_4^+$ and $NO_3^-$, are deposited *via* precipitation scavenging (Wang et al., 2008). The primary loadings on EOF3 are $Ca^{2+}$, $Mg^{2+}$ and $NH_4^+$, which account for 6.2% of the total variance. The difference between the $Ca^{2+}$, $Mg^{2+}$, and $NH_4^+$ time series compared to the time series of other major ions suggests that EOF3 may imply a secondary dust source dominated by $Ca^{2+}$, $Mg^{2+}$ and $NH_4^+$. Dolomite, calcite and magnesite are possible sources of $Ca^{2+}$ and $Mg^{2+}$. For $NH_4^+$, further studies are necessary to clarify whether it is absorbed by dust particles during transportation or whether it is derived from other sources.

Although previous studies have revealed that marine moisture does indeed penetrate the Tanggula region during the summer monsoon season (Tian et al., 2001; Liu et al., 2007) and that interannual changes in $\delta^{18}O$ values in the QT-1 ice core are therefore likely influenced by large scale atmospheric circulations associated with the ENSO cycle (Shao et al., 2017), we did not find an eigenvector that represents sea salt ions within our own EOF analysis. One possible explanation of this finding might be that the precipitation which falls on QT-1 is principally supplied by the Indian Summer Monsoon (ISM), while microparticles are mainly deposited on the glacier's surface during the dry non-monsoon season. Sea salt ions are overwhelmed by abundant crustal inputs after they experience continual scavenging during long-range transport (Li et al., 2007; Zhang et al., 2008). Earlier studies have also indicated that the major ions in the Tanggula ice core are dominated by the chemical compositions of dry depositional materials from local arid areas (Zheng et al., 2010). Local materials account for ~70% of the total atmospheric dust aerosols deposited on the central TP, while materials from remote sources make up the remaining 20–25% (Zhang et al., 1996).

In this study, we focused on EOF1, as this represents the majority of the variance in the major ion concentrations. We compared the EOF1 results with regional dust storm events, meteorological parameters and atmospheric circulation patterns and investigated the environmental significance of the results.

### 3.2. Relationship between EOF1 and dust event records

We made comparisons between the observed dust storm datasets extracted from four nearby stations and one more distant meteorological station (*i.e.*, Gaize, Amdo, Baingoin, Shenzha, and, further afield, Shiquanhe) to investigate the relationship between EOF1 and dust storm events. To remove any potential dating uncertainty, the 5-year running mean values of the EOF1 results were compared to the annual frequency of dust storms (Fig. 3).

Despite the considerable distance (approximately 420 km) between

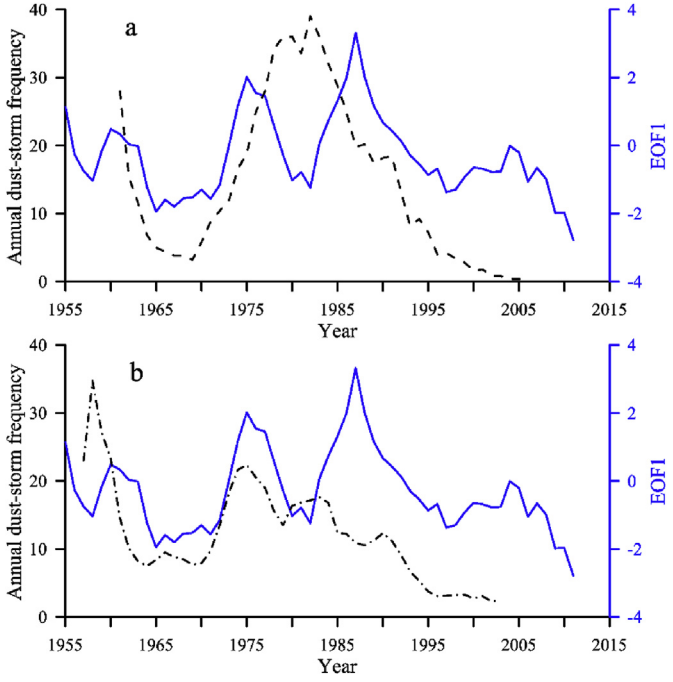


**Fig. 3.** A comparison of the 5-year running means between the EOF1 time series (blue solid line) and: (a) the 47-year time series (1961–2007) derived from the dust storm records of Shiquanhe meteorological station (dashed curve); (b) the 47-year time series (1957–2003) constructed from the composite dust storm records of four nearby meteorological stations (Gaize, Amdo, Baingoin and Shenzha) (dashed dotted curve). (For interpretation of the references to colour in this figure legend, the reader is referred to the Web version of this article.)

**Table 3**
QT-1 EOF1 correlations, GABS: Gaize, Amdo, Baingoin and Shenzha meteorological station. MAP: mean annual precipitation. MAT: mean annual temperature. ASP: atmospheric pressure. WS: wind speed. All correlation analysis was performed after 5-year moving average filter method was applied to EOF1 and climate variables.

| Climate Variable | Period | n | r | p value |
|---|---|---|---|---|
| Shiquanhe dust data | 1961–2007 | 47 | 0.478 | < 0.01 |
| GABS dust data | 1957–2003 | 47 | 0.323 | < 0.05 |
| MAP | 1973–2010 | 38 | −0.435 | < 0.01 |
| MAT | 1973–2010 | 38 | −0.448 | < 0.01 |
| ASP | 1973–2010 | 38 | −0.357 | < 0.05 |
| WS | 1973–2010 | 38 | 0.705 | < 0.01 |
| PDO | 1900–2011 | 112 | 0.321 | < 0.01 |

the QT-1 ice core and Shiquanhe meteorological station, the trends in the variability of EOF1 show a similarity with the dust storm records (Fig. 3a). This is particularly true for the period from 1961 to 1975. This significant correlation (Table 3, $r = 0.478$, $n = 47$, $p < 0.01$) suggests that the ion record is related to dust storm events that have occurred in the western region of the TP. We also constructed a composite dust storm frequency series from four nearby meteorological stations (*i.e.*, Gaize, Amdo, Baingoin and Shenzha, hereafter referred to simply as GABS) to represent a regional scale. Comparative analysis also suggested a robust consistency between EOF1 and the frequency of dust storms as recorded at the GABS meteorological stations (Fig. 3b). EOF1 is also correlated with the dust storm frequency data from the GABS meteorological stations for the time period from 1960 to 1980. Higher EOF1 values and annual layers with larger dust particles centred around the years 1960 and 1975 correlate well with the higher frequency of dust storms observed in these years and recorded by the nearby GABS meteorological stations. Additionally, EOF1 exhibits significant linear correlations with the dust storm records from the GABS meteorological

stations (Table 3, r = 0.323, n = 47, $p < 0.05$). Some discrepancies exist between EOF1 and the dust storm records, *e.g.*, the relatively high frequency of dust storms around 1980 and the comparatively low EOF1 values for this time (Fig. 3), which can probably be explained by the different conditions of the local environments.

The robust correlations noted between the EOF1 values and frequency of dust storms suggests that it is reasonable to assume that QT-1 ion records can provide a proxy for atmospheric dust loading in the central TP. Therefore, according to the EOF1 time series (Fig. 1), over the last century, the 1920–1940, 1950–1960 and 1970–1990 periods were identified to have experienced the highest frequency of dust storms on the central TP. Higher EOF1 values during the 1920–1940 period are also found in the atmospheric dust record of the Tanggula ice core (on the central TP) and Malan ice core (on the northern TP) (Wang, 2005; Wu et al., 2013), as well as in other regions of China (Qian and Zhu, 2001; Liang et al., 2006), indicating that the elevated frequency of dust storms during this period was geographically widespread. After the 1980s, the frequency of dust storms decreased, which can probably be attributed to a reduction in the temperature gradient caused by this asymmetrical warming trend (Qian et al., 2002).

### 3.3. Relationship between EOF1 and meteorological parameters

The annual mean climate data collected between 1973 and 2010 from the GABS meteorological stations were used to analyse possible associations between the meteorological conditions and EOF1. Fig. 4 shows a comparison between the 5-year running means of these meteorological parameters (*i.e.*, temperature, wind speed, precipitation and atmospheric pressure) and EOF1. While the mean annual precipitation (MAP), mean annual temperature (MAT) and atmospheric pressure (ASP) values exhibit significant negative correlations with EOF1 (Table 3, MAP: r = −0.435, $p < 0.01$, n = 38; MAT: r = −0.448, $p < 0.01$, n = 38; and ASP: r = −0.357, $p < 0.05$, n = 38), wind speed (WS) shows a robust positive linear correlation with the EOF1 (Table 3, r = 0.705, $p < 0.01$, n = 38).

Table 3 and Fig. 4 show a significant negative relation between the EOF1 and precipitation. Precipitation is usually one of the factors that determines vegetation growth, which in turn, can protect the topsoil environment and therefore control any fine particles emitted from the soil (Guan et al., 2017), especially in arid and semiarid areas (Wang et al., 2013). Increased levels of precipitation may result in more scavenging and an enhanced soil moisture content, both of which may limit atmospheric dust aerosol loading (Liu et al., 2004a). This would explain why high precipitation correlates with low EOF1 values, and *vice versa*, between 1973 and 2010. For instance, relatively low and fluctuating precipitation levels correspond with relatively high EOF1 values during the period from 1973 to 1995. During 1995–2010, the precipitation levels were much higher and more constant, and, in response, the results for EOF1 appeared comparatively stable, with reasonably lower values.

Previous studies have shown that moderate warming and low atmospheric pressure can reduce the frequency and strength of cyclones and, ultimately, lead to less entrainment of dust within the atmosphere (Qian et al., 2002; Liu et al., 2004a; Zhu et al., 2008). Moderate warming also prolongs the growing season for vegetation, further suppressing the likelihood of dust storms (Guan et al., 2017), which could explain why changes in temperature and atmospheric pressure are negatively correlated with EOF1.

The correlation between WS and EOF1 exhibits the highest correlation coefficient (Table 3, r = 0.705, $p < 0.01$, n = 38), indicating that the ion records in the QT-1 ice core are predominantly controlled by wind intensity. Previous studies have also reported that atmospheric dust aerosols are generated by eolian erosion, uplifted into the middle troposphere, and then transported over long distances by strong prevailing winds (Gillette, 1978; Sun et al., 2001; Guan et al., 2014). During the 1973–2010 period, EOF1 values appear to have decreased and fluctuated less, possibly the result of a gradual reduction in wind speed in most areas of China, except for some areas in central China (Xu

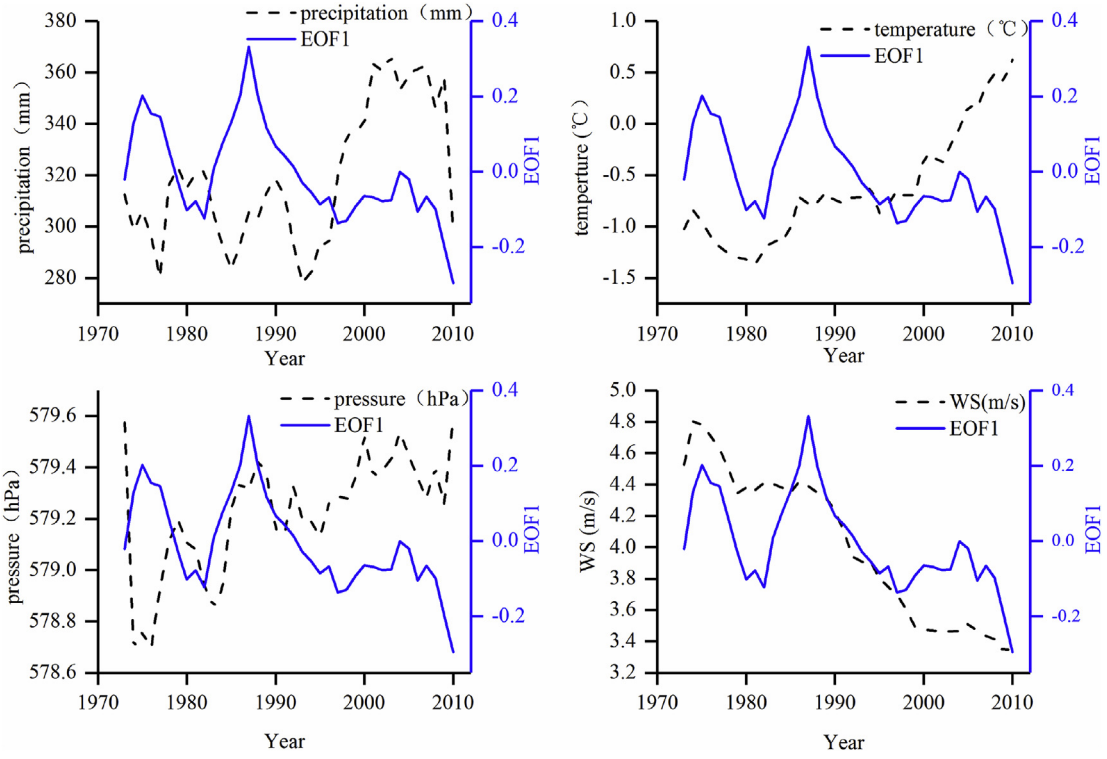


**Fig. 4.** Meteorological parameters (precipitation, atmospheric pressure, wind speed (WS) and temperature) from the GABS meteorological stations (dotted line) and derived from EOF1 (blue line). All values are 5-year running means. (For interpretation of the references to colour in this figure legend, the reader is referred to the Web version of this article.)

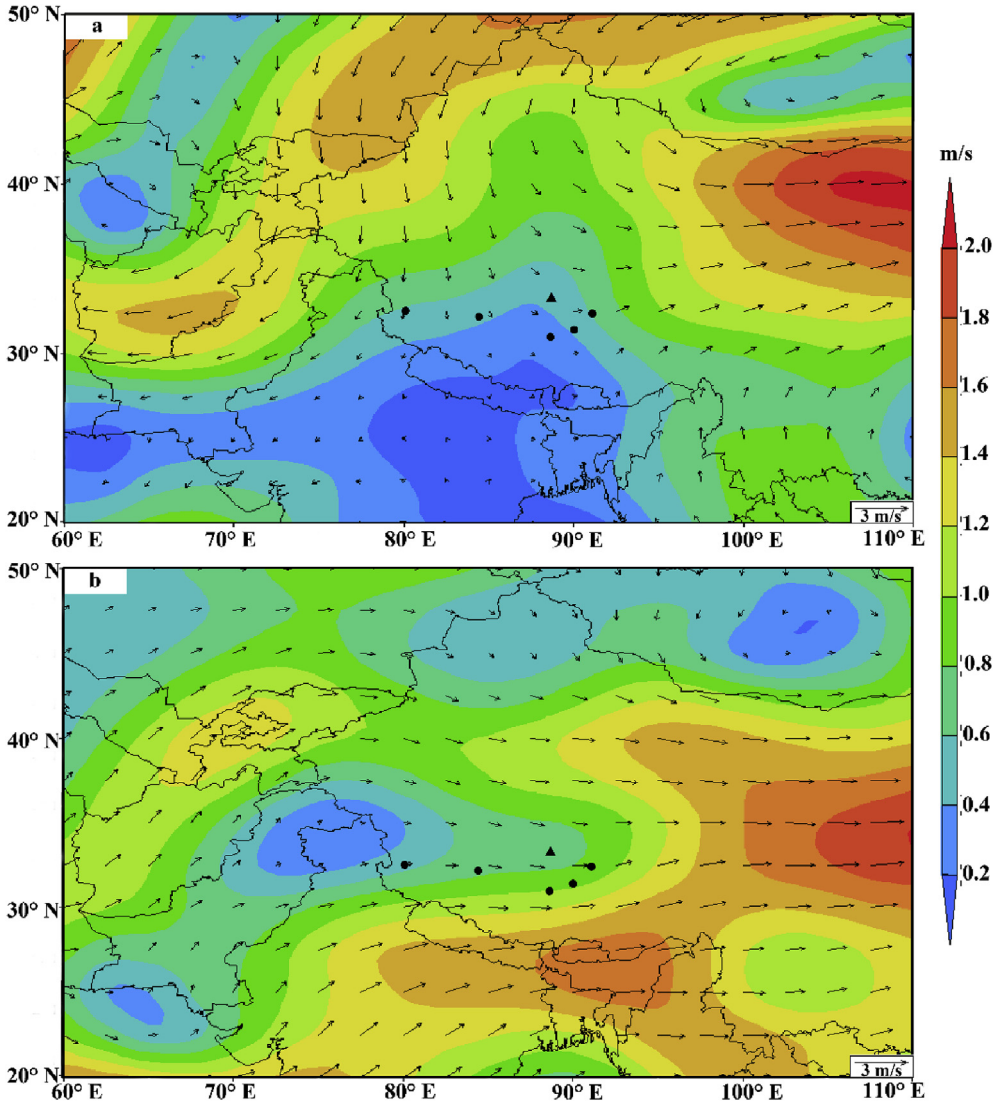


**Fig. 5.** Differences in the 400 hPa monsoon season (a) and non-monsoon season (b) wind vector (m/s) between 1971–1990 (higher EOF1 values) and 1991–2010 (lower EOF1 values). The black triangle represents the QT-1 ice core site, while black dots are the surrounding meteorological stations (from left to right, Shiquanhe, Gaize, Shenzha, Baingoin and Amdo) in each map.

et al., 2006; Jiang et al., 2009; Guo et al., 2011). Furthermore, decreased wind speed has been attributed as a major factor resulting in decreases in surface evaporation (Liu et al., 2004b; Zhang et al., 2007) and is believed to influence the frequency and magnitude of dust storms (Qian et al., 2002; Huang et al., 2006; Yin and Wang, 2007), both of which appear to have influenced, and continue to influence, ion records from the study area.

### 3.4. Relationship between EOF1 and atmospheric circulation patterns

In addition to the regional meteorological parameters mentioned above, atmospheric dust aerosols deposited on ice cores are also affected by large scale anomalous atmospheric circulations which can transport dust aerosols from the arid and semi-arid regions of central Asia (including western China) (Xu et al., 2015; Wake et al., 1993; Wang et al., 2006). Generally, westerlies and frequent dust storms control the climate conditions of the TP during the non-monsoon period (October–May) (Kang et al., 2001; Fang et al., 2004), while during the monsoon season (June–September), the ISM transports moisture and heat northward and penetrates into the northern TP (Tian et al., 2001). Although previous studies showed that dust aerosols on the glacier surface were mainly deposited during the dry non-monsoon season in the central TP (Li et al., 2007; Wu et al., 2013), the anomaly in ionic records may also be attributed to the anomalous atmospheric circulations during the monsoon season. Therefore, to assess the influence of atmospheric circulation patterns on the transportation of atmospheric dust aerosols to QT-1, we performed a composite analysis of 400 hPa winds from the NCEP/NCAR reanalysis data and EOF1 values during non-monsoon period and monsoon period, respectively. We selected the periods from 1971–1990 and 1991–2010, which had relatively high and low annual EOF1 values, respectively, to examine any potential associations between wind speed and EOF1. Fig. 5 shows the difference between the mean seasonal 400 hPa wind field for periods with the higher and lower EOF1 values. Fig. 5a shows that northwesterly winds strengthened during years with higher EOF1 values in monsoon season, suggesting that more of the atmospheric dust aerosols deposited on QT-1 and within the ice core likely originated from the northwestern TP and neighbouring Taklamakan Desert (Wake et al., 1994; Grigholm et al., 2015; Jia et al., 2015; Zhang et al., 2016). Fig. 5b may suggest that the influx of mineral aerosol derived from the central Asia (including western TP) also plays an important role to contribute to the higher EOF1 values in non-monsoon season, which can be transported by the strengthened westerlies (Wake et al., 1993; Wang et al., 2006). Therefore, the results show QT-1 chemical records are also under the

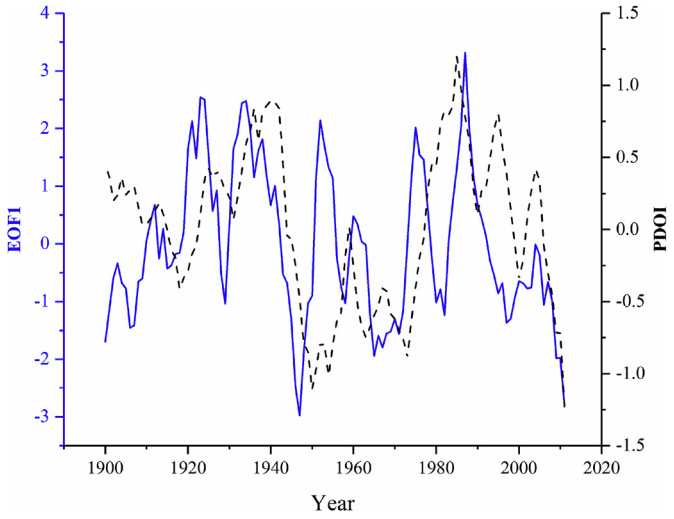


**Fig. 6.** Temporal variations in the PDO index (black dashed curve) and EOF1 (blue solid curve). All values are 5-year running means. (For interpretation of the references to colour in this figure legend, the reader is referred to the Web version of this article.)

influence of the atmospheric circulations which can entrain and transport dust aerosols into the region from the arid and semi-arid regions central of Asia. Moreover, Fig. 5 shows that QT-1 and the surrounding meteorological stations were under the similar type of anomalous atmospheric circulation in both two distinct seasons, which may be a possible reason for the significant correlation between EOF1 and the frequency of dust storms recorded in these meteorological stations.

Therefore, it is reasonable to suggest that the atmospheric dust loading recorded by the QT-1 ice core was, and is, influenced by regional meteorological conditions and atmospheric circulation patterns. As a consequence, the glaciochemical records contained within the QT-1 ice core can be used as proxies for investigating paleoclimatic variability and any changes in atmospheric circulation patterns over the central TP in addition to records for past atmospheric dust loading.

### 3.5. Potential teleconnection with the PDO

A comparison between the annual PDO index and annual EOF1 is shown in Fig. 6. Correlation analysis reveals that the PDO index is significantly positively correlated with the annual EOF1 (Table 3, $r = 0.321$, $p < 0.01$, $n = 112$), suggesting that when SSTs express a positive anomaly over the eastern NPO, more atmospheric dust aerosols may be generated, entrained and deposited on glaciers in the central TP. An EOF analysis of the EOF1 time series and annual PDO index also demonstrate that they share 66% of their variability (*i.e.*, they are positively correlated), equivalent to $p < 0.01$ (Meeker and Mayewski, 2002). This finding suggests that there is teleconnection between EOF1 and the PDO index, similar to findings made during analysis of the Qomolangma ice core (Xu et al., 2014).

The underlying mechanism driving this process is still not clear. The results mentioned above suggested that EOF1 is affected by the regional climate conditions and atmospheric circulation patterns. Therefore, we analysed the anomalies in meteorological parameters and atmospheric circulations in the years with high and low PDO indices, respectively.

Fig. 7 and Table 4 show the regional annual anomalies of atmospheric circulations in 400 hPa and meteorological parameters from the GABS meteorological stations for ten years with high PDO indices (*i.e.*, 1981, 1983, 1984, 1986, 1987, 1992, 1993, 1995, 1997 and 2003) and ten years with low PDO indices (*i.e.*, 1973, 1974, 1975, 1990, 1991, 1999, 2000, 2001, 2008 and 2009), all of which occurred during the period between 1973 and 2010. Fig. 7 shows that in year with positive phase of PDO, the central and western TP were influenced by the slightly enhanced northly winds in monsoon season, while they were controlled by the weakened westerlies in non-monsoon season. It is usually believed that enhanced westerlies can transport more distant dust aerosols to the TP and result in high dust aerosols records (Grigholm et al., 2015; Zhang et al., 2016). Therefore, the results suggest that dust aerosols from other sources (i.e., the northern TP or local sources) rather than the western TP contribute to high EOF1 in the years with high PDO indices.

The data in Table 4 suggest that in years with extremely high PDO indices, wind speeds, atmospheric pressure and EOF1 values were slightly higher, but precipitation and SASMI were lower. These anomalies are in agreement with previous work which have revealed that positive PDO phase can result in the potential failure of the ISM (Krishnan and Sugi, 2003; Krishnamurthy and Krishnamurthy, 2013) and lead to dryness in the marginal regions of China (Li et al., 2004; Ma and Shao, 2006; Fang et al., 2012). We also calculated the mean annual land surface temperature differences between the highest and lowest PDO index years (Fig. 8). The results show that air temperatures over Eurasia are usually lower during PDO warm phases. The atmospheric pressure gradient between the TP and Indian Ocean grows shallower as a result of the lower temperatures over the main Eurasian continent, favouring a weakened ISM but, conversely, causing a strengthening in the influence of continental air masses over QT-1 and its environs (Xu et al., 2014). In addition, these drier and colder climate conditions appear to lead to increases in the atmospheric dust aerosols emitted from the land surface. Coupled with decreases in precipitation, reduced levels of scavenging can further increase the presence of soluble dust particles within the atmosphere during weak ISM seasons.

Therefore, the results suggest that the PDO may exert a significant influence on the glaciochemical records preserved on the central TP by affecting the regional climate conditions which influence the generation of the local dust aerosols and the atmospheric circulation patterns which can transport soluble dust particles from different distant sources.

## 4. Conclusions

The upper part of an ice core from the QT glacier on the central TP provided a history of soluble ions found in glacier ice from 1900 to 2011. Analysis showed that the major soluble ions ($NO_3^-$, $SO_4^{2-}$, $Cl^-$, $K^+$, $Mg^{2+}$, $NH_4^+$, $Ca^{2+}$ and $Na^+$) in the QT-1 ice core most likely originated from crustal aerosols, which had high loadings on EOF1, the eigenvector that represents the highest proportion of the variance in the concentrations of major crustal ions.

EOF analysis also indicated that EOF1 values were consistent with regional dust storm records, suggesting that such storms are a strong driver of the regional atmospheric dust loading identified in the glaciochemical QT-1 ice core records. Calculations of the correlative significance demonstrated that regional meteorological factors (*i.e.*, temperature, precipitation, atmospheric pressure and wind speed) also influenced the EOF1 values. Therefore, the EOF1 likely provides important insights into atmospheric dust aerosol loading and can be used as a proxy for explaining the historical processes of environmental change in the region surrounding the QT glacier. This analysis revealed significantly strengthened northwesterly winds in monsoon season and enhanced westerly winds in non-monsoon season over the western and central TP in higher EOF1 years, suggesting that the glaciochemical records extracted from the QT-1 ice core is associated with atmospheric circulation patterns.

A comparison of the relationship between EOF1 and PDO index values also suggests that large-scale atmospheric circulations may exert a significant impact upon ion records in the QT-1 ice core. When the PDO index was high, a decreased thermal gradient induced a weakened Indian Monsoon, likely creating arid conditions and conditions favourable for the emission, transport and deposition of atmospheric dust aerosols. The ion concentrations recorded in the QT-1 ice core may

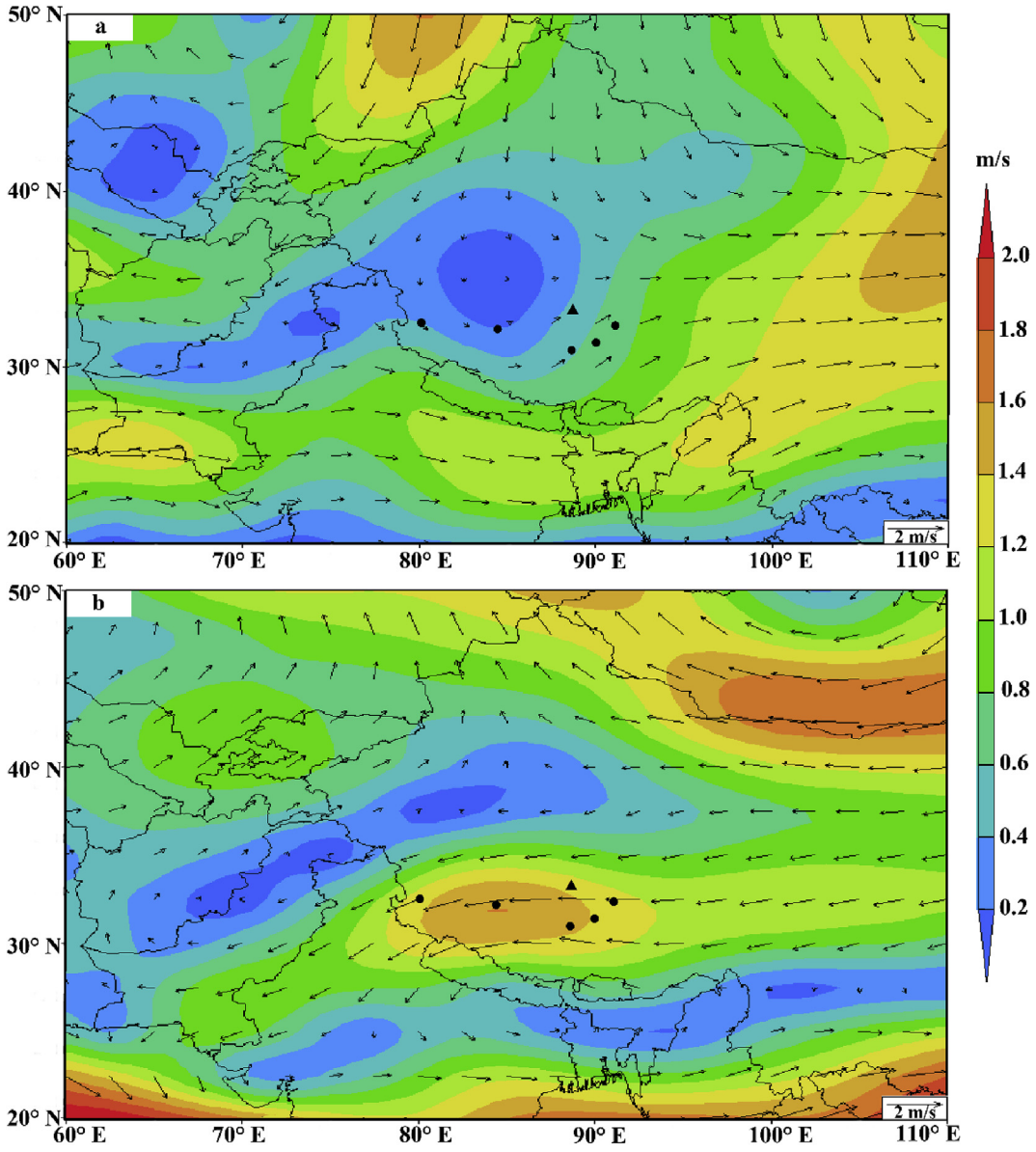


**Fig. 7.** Differences in the 400 hPa monsoon season (a) and non-monsoon season (b) wind vector (m/s) between higher PDO values years and lower PDO values years. The black triangle represents the QT-1 ice core site, while black dots are the surrounding meteorological stations (from left to right, Shiquanhe, Gaize, Shenzha, Baingoin and Amdo) in each map.

**Table 4**
Regional annual anomalies of meteorological parameters over ten years with a relatively high PDO index and ten years with a relatively low PDO index. LST: land surface temperature; SASMI: South Asian Summer Monsoon Index. All numbers represent the mean 10-year values for each parameter.

| PDO phase | PDO value | Precipitation (mm) | Atmospheric pressure (hPa) | Wind speed (m/s) | LST (°C) | EOF1 | SASMI |
|---|---|---|---|---|---|---|---|
| High | 0.97 | −19.75 | 0.02 | 0.02 | −0.41 | −0.29 | −0.41 |
| Low | −0.94 | 19.46 | −0.15 | −0.04 | 0.22 | −0.56 | 0.20 |

further provide a means to reconstruct the PDO, thereby improving understanding of its mechanisms.

## Acknowledgements

This research was funded by the National Natural Science Foundation of China (Grant Nos. 41530748, 41771043 and 41701080) and the China Postdoctoral Science Foundation (Grant 2017M610118). The authors would like to thank the fieldwork team for their work conducted during the summer of 2014. We also gratefully acknowledge the NCEP/NCAR and the National Meteorological Center of the Chinese Meteorological Association (CMA) for the meteorological data used in this research, as well as the Pacific Decadal Oscillation extracted data from http://research.jisao.washington.edu/pdo/, and the South Asian Summer Monsoon index data obtained from http://ljp.gcess.cn/dct/page/65576.

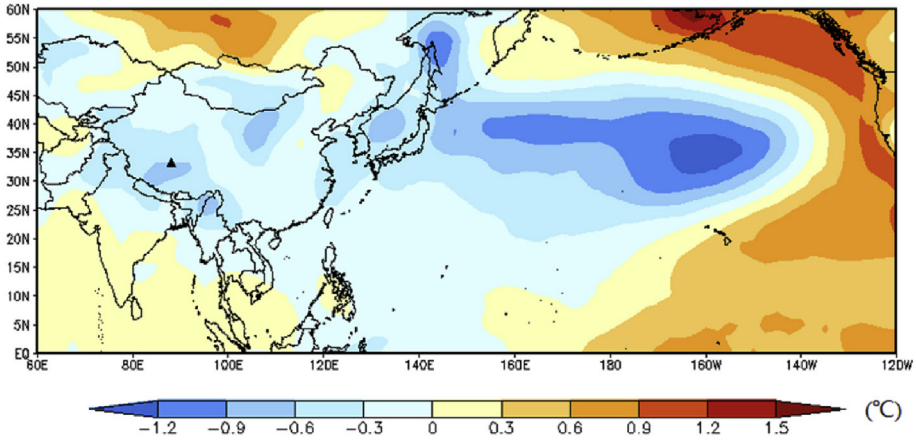


**Fig. 8.** Mean annual surface temperature composite differences for relatively high and low PDO years. The black triangle represents the QT-1 ice core site.

## Appendix A. Supplementary data

Supplementary data to this article can be found online at https://doi.org/10.1016/j.atmosenv.2018.10.028.

## References


Cui, X., Ren, J., Qin, X., Sun, W., Yu, G., Wang, Z., Liu, W., 2014. Chemical characteristics and environmental records of a snow-pit at the glacier No. 12 in the Laohugou valley, Qilian Mountains. J. Earth Sci-China 25 (2), 379–385. https://doi.org/10.1007/s12583-014-0426-6.

Dansgaard, W., Johnsen, S.J., Clausen, H.B., Dahljensen, D., Gundestrup, N.S., Hammer, C.U., Hvidberg, C.S., Steffensen, J.P., Sveinbjornsdottir, A.E., Jouzel, J., Bond, G., 1993. Evidence for general instability of past climate from a 250-kyr ice-core record. Nature 364 (6434), 218–220. https://doi.org/10.1038/364218a0.

Davis, M.E., Thompson, L.G., Yao, T.D., Wang, N.L., 2005. Forcing of the Asian monsoon on the Tibetan Plateau: evidence from high-resolution ice core and tropical coral records. J. Geophys. Res. Atmos. 110 (D4). https://doi.org/10.1029/2004jd004933.

Duan, K., Thompson, L.G., Yao, T., Davis, M.E., Mosley-Thompson, E., 2007. A 1000 year history of atmospheric sulfate concentrations in southern Asia as recorded by a Himalayan ice core. Geophys. Res. Lett. 34 (1), 155–170. https://doi.org/10.1029/2006GL027456.

Fang, K., Gou, X., Chen, F., Frank, D., Liu, C., Li, J., Kazmer, M., 2012. Precipitation variability during the past 400 years in the Xiaolong Mountain (central China) inferred from tree rings. Clim. Dynam. 39 (7–8), 1697–1707. https://doi.org/10.1007/s00382-012-1371-7.

Fang, X.M., Han, Y.X., Ma, J.H., Song, L.C., Yang, S.L., Zhang, X.Y., 2004. Dust storms and loess accumulation on the Tibetan Plateau: a case study of dust event on 4 March 2003 in Lhasa. Chin. Sci. Bull. 49 (9), 953–960. https://doi.org/10.1007/BF03184018.

Gao, C., Robock, A., Ammann, C., 2008. Volcanic forcing of climate over the past 1500 years: an improved ice core-based index for climate models. J. Geophys. Res. 113 (D23). https://doi.org/10.1029/2008jd010239.

Gillette, D., 1978. A wind tunnel simulation of the erosion of soil: effect of soil texture, sandblasting, wind speed, and soil consolidation on dust production. Atmos. Environ. 12 (8), 1735–1743. 1967. https://doi.org/10.1016/0004-6981(78)90322-0.

Grigholm, B., Mayewski, P.A., Kang, S., Zhang, Y., Kaspari, S., Sneed, S.B., Zhang, Q., 2009. Atmospheric soluble dust records from a Tibetan ice core: possible climate proxies and teleconnection with the Pacific Decadal Oscillation. J. Geophys. Res. Atmos. 114 (D20). https://doi.org/10.1029/2008jd011242.

Grigholm, B., Mayewski, P.A., Kang, S., Zhang, Y., Morgenstern, U., Schwikowski, M., Kaspari, S., Aizen, V., Aizen, E., Takeuchi, N., Maasch, K.A., Birkel, S., Handley, M., Sneed, S., 2015. Twentieth century dust lows and the weakening of the westerly winds over the Tibetan Plateau. Geophys. Res. Lett. 42 (7), 2434–2441. https://doi.org/10.1002/2015gl063217.

Grigholm, B., Mayewski, P.A., Aizen, V., Kreutz, K., Aizen, E., Kang, S., Maasch, K.A., Sneed, S.B., 2017. A twentieth century major soluble ion record of dust and anthropogenic pollutants from Inilchek Glacier, Tien Shan. J. Geophys. Res. Atmos. 122 (3), 1884–1900. https://doi.org/10.1002/2016jd025407.

Guan, Q., Yang, J., Zhao, S., Pan, B., Liu, C., Zhang, D., Wu, T., 2014. Climatological analysis of dust storms in the area surrounding the Tengger Desert during 1960–2007. Clim. Dynam. 45 (3–4), 903–913. https://doi.org/10.1007/s00382-014-2321-3.

Guan, Q.Y., Sun, X.Z., Yang, J., Pan, B.T., Zhao, S.L., Wang, L., 2017. Dust storms in northern China: long-term spatiotemporal characteristics and climate controls. J. Clim. 30 (17), 6683–6700. https://doi.org/10.1175/Jcli-D-16-0795.1.

Guo, H., Xu, M., Hu, Q., 2011. Changes in near-surface wind speed in China: 1969-2005. Int. J. Climatol. 31 (3), 349–358. https://doi.org/10.1002/joc.2091.

Hou, S., Qin, D., Zhang, D., Kang, S., Paul A, M., 2003. A 154a high-resolution ammonium record from the Rongbuk Glacier, north slope of Mt. Qomolangma (Everest), Tibet–Himal region. Atmos. Environ. 37 (5), 721–729. https://doi.org/10.1016/S1352-2310(02)00582-4.

Huang, J., Minnis, P., Lin, B., Wang, T., Yi, Y., Hu, Y., Sun-Mack, S., Ayers, K., 2006. Possible influences of Asian dust aerosols on cloud properties and radiative forcing observed from MODIS and CERES. Geophys. Res. Lett. 33 (6), 272–288. https://doi.org/10.1029/2005gl024724.

Jia, R., Liu, Y., Chen, B., Zhang, Z., Huang, J., 2015. Source and transportation of summer dust over the Tibetan Plateau. Atmos. Environ. 123, 210–219. https://doi.org/10.1016/j.atmosenv.2015.10.038.

Jiang, Y., Luo, Y., Zhao, Z., Tao, S., 2009. Changes in wind speed over China during 1956–2004. Theor. Appl. Climatol. 99 (3–4), 421–430. https://doi.org/10.1007/s00704-009-0152-7.

Kang, S.C., Wake, C.P., Qin, D.H., Mayewski, P.A., Yao, T.D., 2000. Monsoon and dust signals recorded in Dasuopu glacier, Tibetan Plateau. J. Glaciol. 46 (153), 222–226. https://doi.org/10.3189/172756500781832864.

Kang, S., Qin, D., Mayewski, P.A., Wake, C.P., Ren, J., 2001. Climatic and environmental records from the Far East Rongbuk ice core, Mt. Qomolangma (Mt. Everest). Episodes 24 176e181.

Kang, S., Mayewski, P.A., Qin, D., Yan, Y., Hou, S., Zhang, D., Ren, J., Kruetz, K., 2002. Glaciochemical records from a Mt. Everest ice core: relationship to atmospheric circulation over Asia. Atmos. Environ. 36 (21), 3351–3361. https://doi.org/10.1016/s1352-2310(02)00325-4.

Kang, S., Zhang, Y., Zhang, Y., Grigholm, B., Kaspari, S., Qin, D., Ren, J., Mayewski, P., 2010. Variability of atmospheric dust loading over the central Tibetan Plateau based on ice core glaciochemistry. Atmos. Environ. 44 (25), 2980–2989. https://doi.org/10.1016/j.atmosenv.2010.05.014.

Kaspari, S., Mayewski, P., Kang, S., Sneed, S., Hou, S., Hooke, R., Kreutz, K., Introne, D., Handley, M., Maasch, K., Qin, D., Ren, J., 2007. Reduction in northward incursions of the South Asian monsoon since ~1400 AD inferred from a Mt. Everest ice core. Geophys. Res. Lett. 34 (16), 880–895. https://doi.org/10.1029/2007GL030440.

Krishnamurthy, L., Krishnamurthy, V., 2013. Influence of PDO on South Asian summer monsoon and monsoon–ENSO relation. Clim. Dynam. 42 (9–10), 2397–2410. https://doi.org/10.1007/s00382-013-1856-z.

Krishnan, R., Sugi, M., 2003. Pacific decadal oscillation and variability of the Indian summer monsoon rainfall. Clim. Dynam. 21 (3–4), 233–242. https://doi.org/10.1007/s00382-003-0330-8.

Legrand, M., Mayewski, P., 1997. Glaciochemistry of polar ice cores: a review. Rev. Geophys. 35 (3), 219–243. https://doi.org/10.1029/96rg03527.

Li, C., He, J., Zhu, J., 2004. A review of decadal/interdecadal climate variation studies in China. Adv. Atmos. Sci. 21 (3), 425–436. https://doi.org/10.1007/bf02915569.

Li, C.L., Kang, S.C., Zhang, Q.G., Kaspari, S., 2007. Major ionic composition of precipitation in the Nam Co region, Central Tibetan Plateau. Atmos. Res. 85 (3–4), 351–360. https://doi.org/10.1016/j.atmosres.2007.02.006.

Li, J.P., Zeng, Q., 2002. A unified monsoon index. Geophys. Res. Lett. 29 (8) 115-1-115-4. https://doi.org/10.1029/2001gl013874.

Li, J.P., Zeng, Q.C., 2003. A new monsoon index and the geographical distribution of the global monsoons. Adv. Atmos. Sci. 20 (2), 299–302. https://doi.org/10.1007/s00376-003-0016-5.

Liang, E.Y., Liu, X.H., Yuan, Y.J., Qin, N.S., Fang, X.Q., Huang, L., Zhu, H.F., Wang, L., Shao, X.M., 2006. The 1920s drought recorded by tree rings and historical documents in the semi-arid and arid areas of Northern China. Climatic Change 79 (3–4), 403–432. https://doi.org/10.1007/s10584-006-9082-x.

Liu, X., Yin, Z.-Y., Zhang, X.Y., Yang, X., 2004a. Analyses of the spring dust storm frequency of northern China in relation to antecedent and concurrent wind, precipitation, vegetation, and soil moisture conditions. J. Geophys. Res. 109 (D16). https://doi.org/10.1029/2004jd004615.

Liu, B., Xu, M., Henderson, M., Gong, W., 2004b. A spatial analysis of pan evaporation trends in China, 1955–2000. J. Geophys. Res. 109 (D15). https://doi.org/10.1029/2004jd004511.

Liu, Z., Tian, L., Yao, T., Yu, W., 2007. Seasonal deuterium excess in Nagqu precipitation:

influence of moisture transport and recycling in the middle of Tibetan Plateau. Environ. Geol. 55 (7), 1501–1506. https://doi.org/10.1007/s00254-007-1100-4.
Ma, Z., Shao, L., 2006. Relationship between dry/wet variation and the Pacific Decadal Oscillation (PDO) in Northern China during the last 100 years. Chin. J. Atmos. Sci. 30 (3), 464–474 (in Chinese).
Mantua, N.J., Hare, S.R., Zhang, Y., Wallace, J.M., Francis, R.C., 1997. A Pacific interdecadal climate oscillation with impacts on salmon production. Bull. Am. Meteorol. Soc. 78 (6), 1069–1079. https://doi.org/10.1175/1520-0477(1997)078<1069:APICOW>2.0.CO;2.
Mayewski, P.A., Lyons, W.B., Ahmad, N., 1983. Chemical-composition of a high-altitude fresh snowfall in the Ladakh Himalayas. Geophys. Res. Lett. 10 (1), 105–108. https://doi.org/10.1029/GL010i001p00105.
Meeker, L.D., Mayewski, P.A., Bloomfield, P., 1995. A new approach to glaciochemical time series analysis. Ice Core Studies of Global Biogeochemical Cycles 30, 383–400. https://doi.org/10.1007/978-3-642-51172-1_20.
Meeker, L.D., Mayewski, P.A., 2002. A 1400-year high-resolution record of atmospheric circulation over the North Atlantic and Asia. Holocene 12 (3), 257–266. https://doi.org/10.1191/0959683602hl542ft.
Newman, M., Alexander, M.A., Ault, T.R., Cobb, K.M., Deser, C., Di Lorenzo, E., Mantua, N.J., Miller, A.J., Minobe, S., Nakamura, H., Schneider, N., Vimont, D.J., Phillips, A.S., Scott, J.D., Smith, C.A., 2016. The Pacific decadal oscillation, revisited. J. Clim. 29 (12), 4399–4427. https://doi.org/10.1175/jcli-d-15-0508.1.
Osterberg, E.C., Winski, D.A., Kreutz, K.J., Wake, C.P., Ferris, D.G., Campbell, S., Introne, D., Handley, M., Birkel, S., 2017. The 1200 year composite ice core record of Aleutian Low intensification. Geophys. Res. Lett. 44 (14), 7447–7454. https://doi.org/10.1002/2017gl073697.
Qian, W., Zhu, Y., 2001. Climate change in China from 1880 to 1998 and its impact on the environmental condition. Climatic Change 50 (4), 419–444. https://doi.org/10.1023/a:1010673212131.
Qian, W.H., Quan, L.S., Shi, S.Y., 2002. Variations of the dust storm in China and its climatic control. J. Clim. 15 (10), 1216–1229. https://doi.org/10.1175/1520-0442(2002)015<1216:Votdsi>2.0.Co;2.
Shao, L.L., Tian, L., Cai, Z.Y., Cui, J.P., Zhu, D., Chen, Y.H., Palcsu, L., 2017. Driver of the interannual variations of isotope in ice core from the middle of Tibetan Plateau. Atmos. Res. 188, 48–54. https://doi.org/10.1016/j.atmosres.2017.01.006.
Shrestha, A.B., Wake, C.P., Dibb, J.E., 1997. Chemical composition of aerosol and snow in the high Himalaya during the summer monsoon season. Atmos. Environ. 31 (17), 2815–2826. https://doi.org/10.1016/S1352-2310(97)00047-2.
Shrestha, A.B., Wake, C.P., Dibb, J.E., Whitlow, S.I., 2002. Aerosol and precipitation chemistry at a remote Himalayan site in Nepal. Aerosol Sci. Technol. 36 (4), 441–456. https://doi.org/10.1080/027868202753571269.
Sun, J., Zhang, M., Liu, T., 2001. Spatial and temporal characteristics of dust storms in China and its surrounding regions, 1960-1999: relations to source area and climate. J. Geophys. Res. Atmos. 106 (D10), 10325–10333. https://doi.org/10.1029/2000jd900665.
Thompson, L.G., Mosley-Thompson, E., Bolzan, J.F., Koci, B.R., 1985. A 1500-year record of tropical precipitation in ice cores from the quelccaya ice cap, Peru. Science 229 (4717), 971–973. https://doi.org/10.1126/science.229.4717.971.
Thompson, L.G., Davis, M., Mosley-Thompson, E., Sowers, T., Henderson, K.A., 1998. A 25,000-year topical climate history from bolivian ice cores. Science 282 (5395), 1858–1864. https://doi.org/10.1126/science.282.5395.1858.
Thompson, L.G., Yao, T., Mosley-Thompson, E., Davis, M.E., Henderson, K.A., Lin, P.A., 2000. A high-resolution millennial record of the south asian monsoon from Himalayan ice cores. Science 289 (5486), 1916–1919. https://doi.org/10.1126/science.289.5486.1916.
Thompson, L.G., Mosley-Thompson, E., Davis, M.E., Zagorodnov, V.S., Howat, I.M., Mikhalenko, V.N., Lin, P.N., 2013. Annually resolved ice core records of tropical climate variability over the past ~1800 years. Science 340 (6135), 945–950. https://doi.org/10.1126/science.1234210.
Tian, L., Masson-Delmotte, V., Stievenard, M., Yao, T., Jouzel, J., 2001. Tibetan Plateau summer monsoon northward extent revealed by measurements of water stable isotopes. J. Geophys. Res. Atmos. 106 (D22), 28081–28088. https://doi.org/10.1029/2001JD900186.
Wake, C.P., Mayewski, P.A., Spencer, M.J., 1990. A review of Central Asian glaciochemical data. Ann. Glaciol. 14, 301–306. https://doi.org/10.3189/S026030550000879X.
Wake, C.P., Mayewski, P.A., Xie, Z.C., Wang, P., Li, Z.Q., 1993. Regional distribution of monsoon and desert dust signals recorded in Asian glaciers. Geophys. Res. Lett. 20 (14), 1411–1414. https://doi.org/10.1029/93gl01682.
Wake, C.P., Dibb, J.E., Mayewski, P.A., Li, Z., Xie, Z., 1994. The chemical composition of aerosols over the eastern Himalayas and Tibetan Plateau during low dust periods. Atmos. Environ. 28 (4), 695–704. https://doi.org/10.1016/1352-2310(94)90046-9.
Wang, N.L., 2005. Decrease trend of dust event frequency over the past 200 years recorded in the Malan ice core from the northern Tibetan Plateau. Chin. Sci. Bull. 50 (24), 2866–2871. https://doi.org/10.1360/982005-237.
Wang, N., Yao, T., Thompson, L.G., Davis, M.E., 2006. Strong negative correlation between dust event frequency and air temperature over the northern Tibetan plateau reflected by the Malan ice-core record. Ann. Glaciol. 43 (1), 29–33. https://doi.org/10.3189/172756406781812339.
Wang, P.L., Yao, T.D., Tian, L.D., Wu, G.J., Li, Z., Yang, W., 2008. Recent high-resolution glaciochemical record from a Dasuopu firn core of middle Himalayas. Chin. Sci. Bull. 53 (3), 418–425. https://doi.org/10.1007/s11434-008-0098-7.
Wang, Y., Shen, Y., Chen, Y., Guo, Y., 2013. Vegetation dynamics and their response to hydroclimatic factors in the Tarim River Basin, China. Ecohydrology 6 (6), 927–936. https://doi.org/10.1002/eco.1255.
Wu, G.J., Zhang, C.L., Xu, B.Q., Mao, R., Joswiak, D., Wang, N.L., Yao, T.D., 2013. Atmospheric dust from a shallow ice core from Tanggula: implications for drought in the central Tibetan Plateau over the past 155 years. Quat. Sci. Rev. 59 (2), 57–66. https://doi.org/10.1016/j.quascirev.2012.10.003.
Xu, C., Ma, Y.M., You, C., Zhu, Z.K., 2015. The regional distribution characteristics of aerosol optical depth over the Tibetan Plateau. Atmos. Chem. Phys. 15 (20), 12065–12078. https://doi.org/10.5194/acp-15-12065-2015.
Xu, H., Hou, S., Pang, H., 2014. Asian–pacific oscillation signal from a Qomolangma (mount everest) ice-core chemical record. Ann. Glaciol. 55 (66), 121–128. https://doi.org/10.3189/2014AoG66A121.
Xu, M., Chang, C.-P., Fu, C., Qi, Y., Robock, A., Robinson, D., Zhang, H.-m., 2006. Steady decline of east Asian monsoon winds, 1969–2000: evidence from direct ground measurements of wind speed. J. Geophys. Res. 111 (D24). https://doi.org/10.1029/2006jd007337.
Yao, T.D., Wu, G.J., Pu, J.C., Jiao, K.Q., Huang, C.L., 2004. Relationship between calcium and atmospheric dust recorded in Guliya ice core. Chin. Sci. Bull. 49 (7), 706–710. https://doi.org/10.1360/03wd0417.
Yin, X.H., Wang, S.G., 2007. Fractal characteristics and trend forecast of duststorms and severe dust-storms in Northern China. J. Desert Res. 27 (1), 130–136 (in Chinese).
Zhang, Q., Kang, S., Wang, F., Li, C., Xu, Y., 2008. Major ion geochemistry of Nam Co lake and its sources, Tibetan plateau. Aquat. Geochem. 14 (4), 321–336. https://doi.org/10.1007/s10498-008-9039-y.
Zhang, W.B., Hou, S.G., An, W.L., Zhou, L.Y., Pang, H.X., 2016. Variations in atmospheric dust loading since AD 1951 recorded in an ice core from the northern Tibetan Plateau. Ann. Glaciol. 57 (71), 258–264. https://doi.org/10.3189/2016AoG71A559.
Zhang, X., Shen, Z., Zhang, G., Chen, T., Liu, H., 1996. Remote mineral aerosols in Westerlies and their contributions to the Chinese loess. Sci. China Earth Sci. 39 (2), 134–143. https://doi.org/10.1360/yd1996-39-2-134.
Zhang, Y., Liu, C., Tang, Y., Yang, Y., 2007. Trends in pan evaporation and reference and actual evapotranspiration across the Tibetan Plateau. J. Geophys. Res. 112 (D12). https://doi.org/10.1029/2006jd008161.
Zhao, H.B., Yao, T.D., Xu, B.Q., Li, Z., Duan, K.Q., 2008. Ammonium record over the last 96 years from the Muztagata glacier in central Asia. Chin. Sci. Bull. 53 (8), 1255–1261. https://doi.org/10.1007/s11434-008-0139-2.
Zhao, H.B., Xu, B., Yao, T., Tian, L., Li, Z., 2011. Records of sulfate and nitrate in an ice core from Mount Muztagata, central Asia. J. Geophys. Res. Atmos. 116 (D13). https://doi.org/10.1029/2011jd015735.
Zheng, M.P., Zhang, Y.S., Liu, X.F., Qi, W., Kong, F.J., Nie, Z., Pu, L.Z., Hou, X.H., Wang, H.L., Zhang, Z., Kong, W.G., Lin, Y.J., 2016. Progress and prospects of salt lake research in China. Acta Geologica Sinica-English Edition 90 (4), 1195–1235. https://doi.org/10.1111/1755-6724.12767.
Zheng, W., Yao, T.D., Joswiak, D.R., Xu, B.Q., Wang, N.L., Zhao, H.B., 2010. Major ions composition records from a shallow ice core on Mt. Tanggula in the central Qinghai-Tibetan Plateau. Atmos. Res. 97 (1–2), 70–79. https://doi.org/10.1016/j.atmosres.2010.03.008.
Zhu, C.W., Wang, B., Qian, W.H., 2008. Why do dust storms decrease in northern China concurrently with the recent global warming? Geophys. Res. Lett. 35 (18), 102. 102. https://doi.org/10.1029/2008gl034886.